Detachable fiber optic tips for use in thulium fiber laser lithotripsy

Thomas C. Hutchens
Richard L. Blackmon
Pierce B. Irby
Nathaniel M. Fried

Detachable fiber optic tips for use in thulium fiber laser lithotripsy

Thomas C. Hutchens,[a] **Richard L. Blackmon,**[a] **Pierce B. Irby,**[b] **and Nathaniel M. Fried**[a,c]
[a]University of North Carolina, Optical Science and Engineering Program, Charlotte, North Carolina
[b]Carolinas Medical Center, Department of Urology, Charlotte, North Carolina
[c]Johns Hopkins Medical Institutions, Department of Urology, Baltimore, Maryland

Abstract. The thulium fiber laser (TFL) has recently been proposed as an alternative to the Holmium:YAG (Ho:YAG) laser for lithotripsy. The TFL's Gaussian spatial beam profile provides higher power transmission through smaller optical fibers with reduced proximal fiber tip damage, and improved saline irrigation and flexibility through the ureteroscope. However, distal fiber tip damage may still occur during stone fragmentation, resulting in disposal of the entire fiber after the procedure. A novel design for a short, detachable, distal fiber tip that can fit into a ureteroscope's working channel is proposed. A prototype, twist-lock, spring-loaded mechanism was constructed using micromachining methods, mating a 150-μm-core trunk fiber to 300-μm-core fiber tip. Optical transmission measuring 80% was observed using a 30-mJ pulse energy and 500-μs pulse duration. *Ex vivo* human calcium oxalate monohydrate urinary stones were vaporized at an average rate of 187 μg/s using 20-Hz modulated, 50% duty cycle 5 pulse packets. The highest stone ablation rates corresponded to the highest fiber tip degradation, thus providing motivation for use of detachable and disposable distal fiber tips during lithotripsy. The 1-mm outer-diameter prototype also functioned comparable to previously tested tapered fiber tips. © *The Authors. Published by SPIE under a Creative Commons Attribution 3.0 Unported License. Distribution or reproduction of this work in whole or in part requires full attribution of the original publication, including its DOI.* [DOI: 10.1117/1.JBO.18.3.038001]

1 Introduction

1.1 Current Laser Lithotripsy Techniques

It is estimated that 10% of the United States population will suffer from urinary stone disease during their lifetime. The National Institute of Diabetes and Digestive and Kidney Diseases (NIDDK) reports that more than 1 million cases occur annually, and billions of dollars are spent on evaluations and treatments each year.[1] To treat severe urinary stone disease an endoscopic laser approach is commonly used with an optical fiber inserted into the working channel of an ureteroscope, which stretches from the urethra to the stone's location in the bladder, ureter, or kidney. The Holmium:YAG (Ho:YAG) laser is currently the laser of choice among urologists because it is a multipurpose system that can be used to cut or coagulate a variety of soft and hard tissues, and because of its relatively low cost, high power output, and the high water absorption in tissue at its emission wavelength of 2120 nm. The Ho:YAG laser, with a pulse duration in the 100 s of microseconds produces a predominantly photothermal laser-tissue interaction mechanism.[2]

Limitations of the Ho:YAG laser include a relatively large and multimode beam waist as well as limited flexibility in operating parameters like pulse duration and pulse rate. Due to space limitations in the single working channel of the flexible ureteroscope, which has a 1.2-mm inner-diameter (ID), 270-μm-core fibers or smaller are used for improved irrigation and higher

flexibility, especially for accessing hard-to-reach locations in the lower pole of the kidney. However, optical coupling into these smaller fibers with the Ho:YAG laser's multimode beam profile risks overfilling of the input fiber core, launching into the cladding, and damaging the fiber. The Ho:YAG laser's large beam waist prevents optimal power coupling into optical fibers smaller than 270 μm.[3] Thermal lensing with the Ho:YAG laser is also a concern, potentially leading to misalignment of the laser beam with the fiber input end.[4] The short bending radius in the distal end of the ureteroscope further decreases the longevity of 270-μm fibers due to laser energy leaking from the core into the cladding, and potentially damaging the ureteroscope. Suboptimal coupling from the large multimode beam profile and stone fragmentation can damage the fiber on the proximal and distal ends, respectively, and the fiber must then be replaced.

Single use and reusable fibers are available for Ho:YAG laser lithotripsy, with 270- and 365-μm fibers as the most common for use in flexible or semirigid ureteroscopes, respectively. Reusable fibers have their jacket stripped, tip cleaved, and are sterilized after each procedure. This reprocessing cost is minimal compared to the cost of a single use fiber. Reusable fibers are usually discarded when they become too short, or if they are irreparably damaged from bending or suboptimal coupling. Reusability of Ho:YAG laser lithotripsy fibers have been reported to decrease single procedure cost by an average of $100 US Dollars.[5]

1.2 Thulium Fiber-Laser Lithotripsy

The experimental thulium fiber laser (TFL) has recently been studied as an alternative laser lithotripter to the clinical Ho:YAG laser for several reasons.[6–11] First, the TFL has a higher

Address all correspondence to: Nathaniel Fried, University of North Carolina at Charlotte, Department of Physics and Optical Science, 9201 University City Boulevard, Charlotte, North Carolina 28223. Tel: 704-687-8149; Fax: 704-687-8197; E-mail: nmfried@uncc.edu

absorption coefficient (160 cm^{-1}) and shorter optical penetration depth in water, which in part translates into a four-time lower ablation threshold for the TFL compared with the Ho:YAG (28 cm^{-1}).[11–13] This, in turn, allows the TFL to ablate tissues at lower pulse energies than with the Ho:YAG laser. Although urinary stones have significantly less bound water content than soft tissues, the urinary stone is typically immersed in a fluid environment and saline irrigation is used to improve visualization during lithotripsy so that unbound water is also present. Experiments have shown a wavelength dependant correlation in ablation threshold to water absorption between Ho:YAG and TFL.[6] The TFL has two major emission wavelengths at 1908 and 1940 nm, which closely match both a high and low temperature water absorption peak, respectively. Its absorption peak shifts from 1940 nm at room temperature to 1910 nm at higher temperatures encountered when the water is superheated during laser tissue ablation.[13–15]

The diode-pumped TFL can also be electronically triggered to operate at nearly any pulse length or configuration, unlike the flashlamp-pumped Ho:YAG laser, which, in general, is limited to lower pulse rates and fixed pulse lengths. Micropulse trains, or pulse packets, have been reported to increase laser ablation rates for both soft tissues[16,17] and hard tissues, including urinary stones.[9] In this study, pulse packet configurations along with standard pulse rates will be used to compare stone ablation rates of a detachable fiber tip design to recent tapered fiber studies.

Another advantage of the TFL is its Gaussian spatial beam profile compared to the Ho:YAG laser's multimode beam. The superior spatial beam profile of the fiber laser improves coupling and transmission of laser power through small-core fibers for lithotripsy, allowing use of core diameters less than 200 μm.[7] This reduction in fiber cross-section allows for increased ureteroscope deflection and higher saline irrigation rates through the working channel,[8,18] which, in turn, may reduce procedure times and probability of ureteroscope damage, and improve patient safety. However, smaller diameter distal fiber tips have been shown to degrade and suffer from "burn-back" more than larger diameter fiber tips.[8,19]

1.3 Tapered Distal Fiber Tips

Tapered fibers have a core diameter that changes linearly along its length.[20] The taper can be gradual along the entire fiber length or steep at one of the tips. Proximal tapered fiber tips have been used to more efficiently couple Ho:YAG laser energy into fibers with smaller trunk diameters. However, higher order modes are created once the small core size is reached at the distal end of the taper. These modes fall outside the total internal reflection condition of the fiber and escape into the fiber cladding, potentially degrading fiber integrity. With extremely tight bending of the fiber, such as with ureteroscope deflection into the lower pole of the kidney, these leaking modes may increase, escape, and burn through the ureteroscope wall, damaging the ureteroscope and potentially harming the patient as well.

The TFL's Gaussian beam profile provides improved coupling into small fibers, eliminating proximal fiber tip damage.[7] By reversing the typical orientation of the tapered fiber, and using the increasing taper and larger core at the output end, the distal fiber tip is more damage resistant during lithotripsy.[8] The benefits of a small core trunk fiber including increased irrigation and flexibility are then combined with that of a robust large core distal fiber tip. The tip (Fig. 1) can be extruded
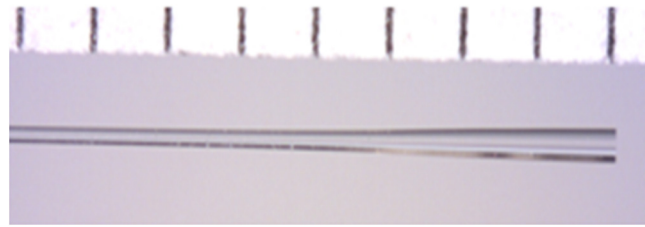

Fig. 1 Tapered fiber distal tip used for comparative studies. Core diameter increases from 150 to 300 μm over 5 mm. Scale in millimeters.

from the ureteroscope into contact with the stone, while also providing sufficient irrigation since only the small diameter trunk fiber remains within the working channel.

Other potential advantages of a tapered distal fiber tip include less divergence of the output beam and a larger treatment area. However, fiber tip damage and burn-back may still occur with large tips and the entire fiber must be replaced or repaired during or after the procedure. Since the TFL eliminates proximal end damage, a detachable and disposable large-core distal fiber tip may improve fiber longevity, procedure performance, and customization of laser lithotripsy. This study will show similar performance between the tapered distal fiber tip[8] and a novel small-core trunk fiber to large-core detachable fiber tip design for TFL lithotripsy.

1.4 Detachable Fiber Tips

Fiber-to-fiber connectors have been available for decades and are standard in the telecommunications industry. Fiber connectors have also been used in laser medicine to easily replace and self-align the proximal end of a fiber with the laser system for surgical applications. Connectorized fibers are commercially available with cleaved, tapered, diffusing, or side-firing distal tip geometry for laser surgery. However, standard fiber-to-fiber mating sleeves are too large and rigid for use within a flexible ureteroscope. To join two fibers, or attach a large core distal fiber tip with a profile of less than 1-mm diameter, splices, capillaries, and hypodermic tubing have been used. However, these are permanent constructs with no simple method to manually detach and replace tips like the large standardized connectors. A small air gap between the trunk and tip fibers has also shown to reduce coupling damage for high power applications.[21]

This study introduces a novel, low-profile, easily detachable distal fiber tip interface for potential use in laser lithotripsy. A prototype device was designed, constructed, and tested in the laboratory.

2 Materials and Methods

2.1 Laser and Tapered Fiber

An electronically modulated, continuous wave 100-W TFL (TLR 110–1908, IPG Photonics, Oxford, Massachusetts) with a center wavelength of 1908 nm was used. Average laser power was measured with a power meter (Powermax PM10, Coherent, Santa Clara, California) and then divided by pulse rate to obtain pulse energy. A 75-mm-focal-length calcium fluoride (CaFl) lens focused the 5.5-mm-diameter collimated laser beam to a 75-μm ($1/e^2$) spot for coupling into the 150-μm-core trunk fiber of the detachable fiber system and tapered fiber. The 2-m-long tapered fiber, used for comparative studies, had a 150- to 300-μm-core taper over a 5-mm length at the
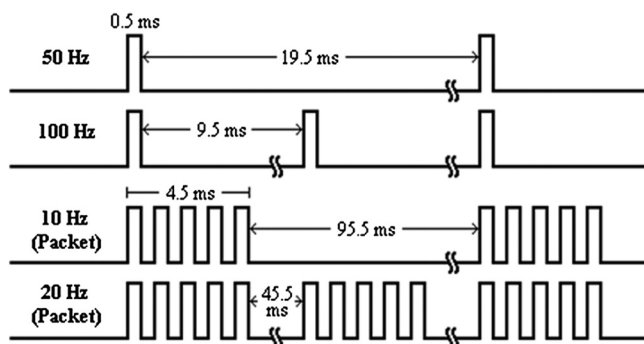
Fig. 2 Diagram showing standard (50 and 100 Hz) pulse trains compared to pulse packets (10 and 20 Hz).

distal tip (FIPE150165195, Polymicro, Phoenix, Arizona), shown in Fig. 1.

The laser was electronically modulated with a function generator (DS345, Stanford Research Systems, Sunnyvale, California) to produce various pulse rates and profiles for device performance testing during stone ablation. For these studies, 500-μs pulses at standard pulse rates of 50 and 100 Hz were compared to 10 and 20 Hz pulse packets consisting of five 500-μs pulses with a 50% duty cycle. These four pulse profiles are shown in Fig. 2, and will be referred to as 50, 100, 10 (Packet), and 20 (Packet) Hz. The 50- and 10-Hz (Packet) pulse profiles contain the same number of total pulses per second, as do the 100 and 20-Hz (Packet) profiles; however, micropulse trains have been shown previously to increase stone ablation rates roughly by a factor of two over the equivalent standard pulse configuration.[9]

2.2 Detachable Fiber Tip Design

Three major constraints were considered when designing the detachable fiber tip interface. First, the design must be 1 mm or smaller in diameter to fit into the working channel of a standard flexible ureteroscope. Second, the detachable mechanism must be simple for an urologist to rapidly interchange fiber tips in the clinic. Third, the design fabrication must be practical with the potential to be mass produced at low cost.

A spring-loaded, twist-locking design, shown in Fig. 3, was built because it satisfied all of the design constraints. A trunk fiber was fitted with a spring with a 400-μm ID and 600-μm OD. The spring was the main dimensional design constraint as it was the smallest spring available. The dimensional designs were based on a low-OH silica trunk fiber with 150-μm-core diameter and 2-m length, which was chosen because it had

identical trunk fiber characteristics as the tapered fiber for comparison. The 300-μm-core fiber tips were of the same material and manufacturer. Hypodermic stainless steel and polyimide tubing was cut and shaped to suit the two fibers and spring to provide concentric structure. The detachable tip "key" was made of 36-gauge wire. Table 1 summarizes the detachable fiber tip components used in the design.

Cleaving the fiber tips would be satisfactory for surgery; however, for consistency, the fiber tip ends were instead polished using 0.3-μm-grit aluminum oxide pads (Buehler, Lake Bluff, Illinois). All components were sealed and secured together with a conservative amount of super glue (Loctite, Westlake, Ohio). Only one piece of tubing, the J-groove, needed careful machining to provide a channel for the key, shown in Fig. 4. A 125-μm diameter end mill bit (05EM013-2-070FL, Drill Bit City, Prospect Heights, Illinois) along with a tabletop vertical milling drill (MicroLux, Micro-Mark, Berkeley Heights, New Jersey) were used with $x - y - z$ micromanipulation stages under magnification to cut the J-groove channel in hypodermic tubing. The design provided a small air gap between the trunk fiber and distal fiber tip, controlled by the length of the locking notch in the J-groove which was 0.3 mm. The distal fiber piece had to remain close to the trunk fiber so that the optical divergence from the trunk fiber did not overfill the fiber tip's proximal end. The stainless steel cover, originally with a 1.27-mm OD, was filed down to 1.00-mm OD to fit inside a typical flexible ureteroscope working channel with a 1.19-mm ID. The overall insertion distance of the tip was 5 mm followed by a 0.3-mm return after 90-deg. clockwise rotation and release. With the trunk fiber tip barely recessed beyond the J-groove cut and the proximal end of the detachable tip flush with the edge of the locking key, the trunk-to-tip air gap was 0.3 mm, or the length of the locking notch. The detachable tip mechanism that fell above the 200-μm OD trunk fiber, shown in Fig. 5(a) with the tip attached, had an overall length of 10 cm with only 2 cm of that region rigid around the fiber interface, with an overall 1-mm OD. The polyimide tubing and thin steel tubing on the trunk fiber were flexible. The entire detachable system (10-cm length) was manually deflected up to 45 degs. without optical transmission failure, demonstrating that the trunk/tip interface design provided efficient laser beam coupling without misalignment under bending conditions.

2.3 Optical and Thermal Characterization

Optical transmission efficiency tests were performed by measuring pulse energy at locations before the trunk fiber tip and after the distal fiber tip, for both detachable and tapered fibers. A thermal imaging camera (Thermovision A20M, FLIR Systems, Boston, Massachusetts) was used to acquire temperature profiles of the detachable fiber tip interface and tapered fiber during laser transmission. Spatial beam profile measurements were acquired by magnifying the fiber tip's surface with a 0.5-numerical aperture (NA) CaFl magnification lens (ISP Optics, Irvington, New York) onto an infrared beam profiler (Pyrocam III, Spiricon, Logan, Uttah). The beam profiler was also used without a magnification lens at incremental distances to analyze the NA of each fiber tip.
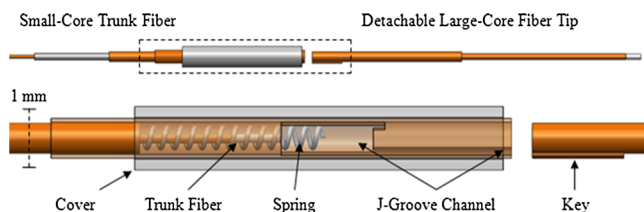

Fig. 3 Detachable fiber tip design with spring-loaded, twist-locking mechanism. The trunk fiber contains the locking mechanism while the distal tip is simply outfitted with a keyed sleeve. (Top) Overall interface and detachable tip. (Bottom) Magnified twist locking region with transparent tubing to see internal geometry.

2.4 Lithotripsy Setup

To compare stone ablation rates of the detachable fiber tip to recent tapered fiber tip studies, human calcium oxalate

Table 1 Materials used to assemble detachable fiber optic tip prototype. All dimensions for inner (ID), outer diameter (OD), and cut length are in millimeters.

	Part	ID (mm)	OD (mm)	Length (mm)	Part #
Trunk	Fiber	n/a	0.195	2,000	FIP150165195 (PM)
	Tubing (S)	0.203	0.414	50	B00137POT6 (AS)
	Tubing (P)	0.455	0.607	40	B000FN4422 (AS)
	Spring	0.400	0.600	4	CIM010ZA 05S (LS)
	J-groove tubing (P)	0.643	0.795	25	B0013HUD9M (AS)
	Cover tubing (S)	0.838	1.270ª	20	B000FN0VNS (AS)
Tip	Fiber	n/a	0.370	50	FIP300330370 (PM)
	Tubing (P)	0.455	0.607	15	B000FN4422 (AS)
	Key	n/a	0.125	2.5	Wire-MW-36-1/4 (PW)

Note: (S) Stainless steel, (P) Polyimide, (ID) Inner diameter, (OD) outer diameter, (n/a) not applicable, (PM) Polymicro, Phoenix, AZ, (AS) Amazon Supply, Seattle, WA, (LS) Lee Spring, Greensboro, NC, (PW) Powerwerx, Brea, California
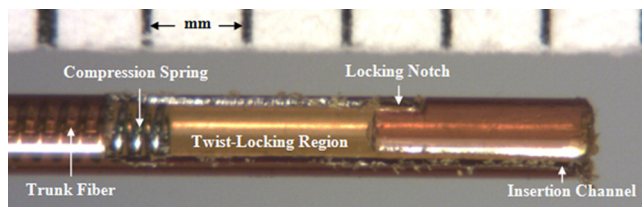ªFiled down to an OD of ~1.00 mm

Fig. 4 Photograph of detachable fiber tip twist-locking mechanism or "J-groove" with outer cover removed.
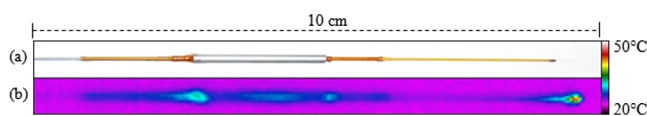

Fig. 5 (a) Photograph of detachable fiber optic tip prototype with outer diameter (OD) of 1.00 mm. (b) Thermal image of prototype in air operating at a 30-mJ pulse using 20 Hz (Packet) pulse profile.

monohydrate (COM) urinary stone samples with >95% purity were obtained from a stone analysis lab (Louis C. Herring, Orlando, Florida). Stone samples ranged from 8 to 15 mm in diameter, and 150 to 500 mg in mass, with an average mass of 250 mg. Initial dry stone mass was recorded with an analytical balance (AB54-S, Mettler-Toledo, Switzerland) before securing the stone in place with a clamp and submerging it into a saline bath. Figure 6 shows the experimental setup. A laser pulse energy of 30 mJ was delivered through the detachable or tapered fiber tips to the stone surface in contact mode. The fiber was held manually and gently scanned over the stone surface during laser irradiation to keep the fiber in constant contact with the stone. A total of 6000 pulses were delivered to each stone sample, for a total ablation time of 1 or 2 min with 100 or 50 pulses per second, respectively. The stones were then dried in an oven at 70°C for over 30 min before final dry mass measurements.
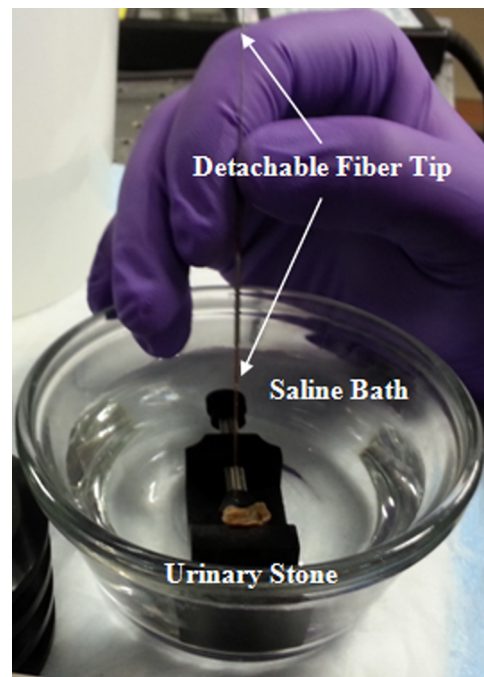

Fig. 6 Laser lithotripsy setup consists of a human calcium oxalate monohydrate (COM) urinary stone submerged in a saline bath with the detachable fiber tip or the tapered fiber tip held manually in contact with the stone surface during laser irradiation.

2.5 Fiber Tip Degradation

The primary motivation for using detachable fiber tips is the observation that the distal tip degrades or experiences burn-back during stone fragmentation. Two fiber degradation studies were performed to study the trends and causes of fiber burn-back. First, microscopic images of the distal fiber tips were taken after stone ablation to analyze fiber burn-back as a function of laser pulse rate and temporal pulse configuration. The

detachable fiber tips and tapered fibers were illuminated with a white light lamp from the proximal end.

Comparison of fiber tip roughness to the number of pulses during stone ablation was also performed because the short length detachable fiber tips in a vertical orientation could easily fit under, and be measured with, a tabletop interferometer. Surface roughness measurements were performed using a scanning white light interferometer, SWLI, (ZeGage, Zygo Corp., Tucson, Arizona) and a 50× magnification objective. A spherical fit to the profile was removed because the fiber tips were slightly convex (2-μm center cladding) because of the fiber polishing machine. The fiber was initially polished and measured, then re-measured after stone ablation to analyze fiber tip roughness.

3 Results

3.1 Optical and Thermal Measurements

For the detachable fiber tip, the measured input and output pulse energy was 38.4 and 30.7 mJ, respectively, yielding a 79.9% transmission. Tapered fiber output pulse energy measured 35.2 mJ for the same input energy, yielding a 91.7% transmission. The detachable fiber tip had four silica/air interfaces while the tapered fiber tip only had two, which may be responsible, in part, for this difference. Theoretical optical transmission rates for the detachable and tapered fiber tips were calculated to be 87.3% and 93.3%, respectively, based on a Fresnel reflection loss of 3.25% at each silica ($n = 1.44$)/air ($n = 1$) interface and a reported 0.014 dB attenuation through a 2-m-long fiber at $\lambda = 1908$ nm.

Table 2 shows lateral thermal imaging and temperature measurements of the detachable fiber tip mechanism and tapered distal fiber tip during laser emission. Figure 5(b) shows a thermal image taken of the detachable fiber tip during laser operation with 30-mJ pulse energy at the 20 Hz (Packet) pulse configuration. When scaled based on pulse configuration, all thermal images showed heating at similar locations. Temperature rise in both fibers was dependent on total pulses per second rather than pulse configuration (standard or packets).

Spatial beam profiles magnified at the fiber tip's surface for the 150 to 300-μm-core diameter detachable fiber tip and the similarly sized tapered fiber are shown in Fig. 7. The detachable fiber tip displayed a Gaussian-like profile, while the tapered fiber had a more unique flatter profile with rings. An experimental numerical aperture was calculated by measuring beam radii at various distances from the distal fiber tip using a spatial beam profiler. With the proximal fiber launching condition kept
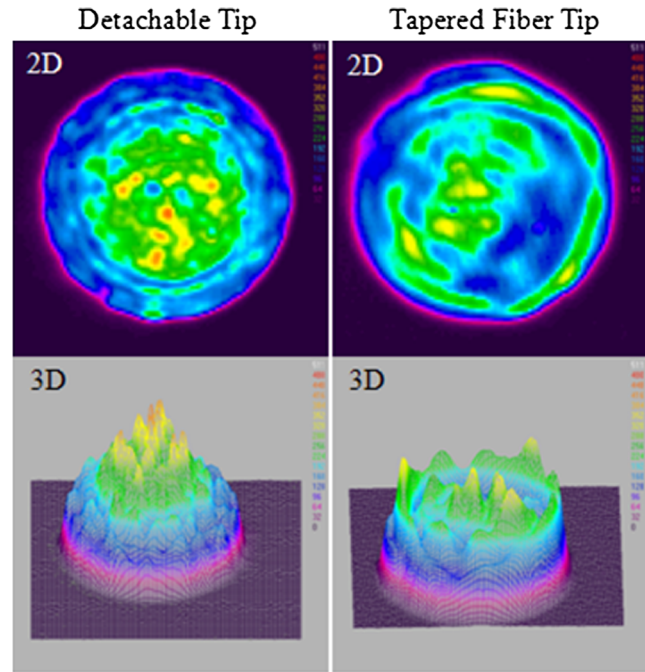

Fig. 7 Distal fiber tip spatial beam profiles for detachable and tapered fiber tips.

common at a NA of 0.037, the detachable and tapered fiber tips had output NAs of 0.078 and 0.055, respectively.

3.2 Lithotripsy

COM stones were ablated with the detachable fiber tip at a maximum rate of 187 μg/s using the 20-Hz (Packet) pulse profile at 30 mJ. Table 3 shows the mean ablation rate based on five stone samples for each set of laser parameters. The stones were not fragmented into smaller stones by the laser, but rather all stone mass loss was the result of stone vaporization with particle sizes less than 100 μm. Contrary to the temperature rise results, stone ablation rates for both fibers tended to favor the pulse packets rather than the standard pulse rates. A Student's t-test showed no statistical difference between detachable and tapered fiber stone ablation rates.

3.3 Fiber Tip Degradation

Degradation of the detachable fiber tip was studied in two ways. First, microscopic images of the fiber tips after stone ablation

Table 2 Peak temperature and temperature rise of detachable and tapered fiber tips as a function of laser temporal pulse profile.

Pulse profile	Pulses/s	Detachable tip*		Tapered tip*	
		Interface (°C)	Distal Tip (°C)	Trunk Jacket (°C)	Distal Tip (°C)
50 Hz	50	30.1 (Δ5.5)	36.1 (Δ11.5)	26.0 (Δ2.6)	25.3 (Δ1.9)
10 Hz (Packet)	50	27.8 (Δ3.2)	37.4 (Δ12.8)	26.1 (Δ2.7)	25.9 (Δ2.5)
100 Hz	100	31.2 (Δ6.6)	48.5 (Δ23.9)	28.4 (Δ5.0)	27.3 (Δ3.9)
20 Hz (Packet)	100	33.5 (Δ8.9)	47.0 (Δ22.4)	28.7 (Δ5.3)	27.8 (Δ4.4)

*Mean room temperature for detachable (24.6°C) and tapered (23.4°C) fiber measurements. Pulse energy: 30 ± 2 mJ.

Table 3 Calcium oxalate monohydrate (COM) stone ablation rates for detachable and tapered fiber tips as a function of laser pulse rate and profile.

Pulse profile	Pulses/s[*]	Detachable tip (μg/s)	Tapered tip (μg/s)
50 Hz	50	50 ± 15	47 ± 9
10 Hz (Packet)	50	108 ± 13	94 ± 22
100 Hz	100	113 ± 8	92 ± 37
20 Hz (Packet)	100	187 ± 37	175 ± 31

*Rates calculated from mass loss after 6000 pulses ($N = 5$). Pulse energy: 30 ± 2 mJ.

were taken (Fig. 8). Minimal degradation was observed for 50 Hz, while the 100 and 10 Hz (Packet) profiles showed signs of pitting. Significant burn-back was seen at 20 Hz (Packet) for both detachable and tapered fiber tips. This trend was consistent with the stone ablation rates. Second, to better understand the fiber burn-back mechanism a more rigorous fiber tip roughness analysis was also performed. Figure 9 shows the measured fiber tip roughness before and after delivery of 60,000 total laser pulses at 50 Hz. This was equivalent to 20 min, or five times longer than the 12,000 pulse tip degradation image for 50 Hz in Fig. 8. The root-mean-squared (Rq) roughness parameter only changed from 4.72 to 4.77 nm, and the average roughness (Ra) changed from 3.35 to 3.48 nm, essentially identical.

4 Discussion

4.1 Detachable Fiber Tip Design

The detachable fiber tip prototype has a much smaller diameter and is more flexible than commercial fiber connectors. The overall device diameter of 1.00 mm (3.0 Fr) is slightly smaller than a typical flexible ureteroscope working channel diameter of 1.19 mm (3.6 Fr). However, the design itself could easily be scaled down further if a smaller spring was available. If the J-groove part was reduced in diameter, it would need to be machined from stainless steel tubing because the polyimide tubing would be too flexible at these small diameters and the
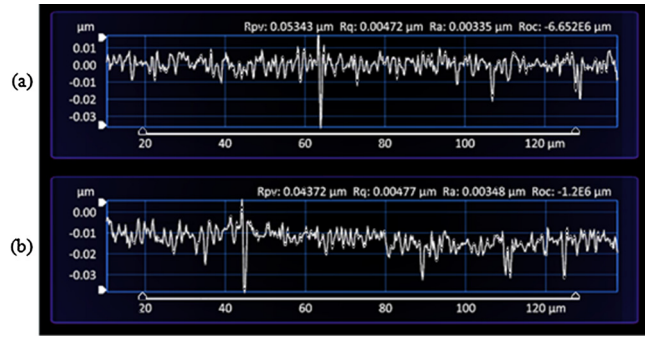

Fig. 9 Distal fiber tip roughness measurement using a scanning white light interferometer. (a) Polished and before lasing, root-mean-squared (Rq) = 4.72 nm, average roughness (Ra) = 3.35 nm. (b) After 60,000 500-μs pulses at a standard pulse rate of 50 Hz, with a pulse energy of 30 mJ, Rq = 4.77 nm, Ra = 3.48 nm. The peak-valley (Rpv) and radius-of-curvature (Roc) parameters given by the analysis software (ZeMaps) are not significant parameters because they are primarily dependent on singular features and form removal, respectively.

J-groove cut would need to support the pressure of the spring and multiple tip exchanges with consistency. The long length of the current prototype was to aid in the manual grasping of the device in the *ex-vivo* stone ablation testing, as shown in Fig. 6. The cut lengths of all the device components, as shown in Table 1, could be reduced to increase the overall flexibility for use inside the ureteroscope working channel, and to insert the fiber through the working channel during the procedure without hindering ureteroscope deflection. The cyanoacrylate-based "superglue" used in this preliminary study could also be replaced by a heat-resistant biocompatible glue, thus making it acceptable for clinical use and re-sterilization, if necessary.

4.2 Optical and Thermal Analysis

Both the detachable and tapered fiber tips performed within 90% of their theoretical optical transmissions. Minor discrepancies may lie in the proximal coupling, polishing artifacts, or in the case of the detachable fiber tip, debris from construction or suboptimal concentricity between the trunk and tip fibers. However, the overall optical transmission for both fibers should increase when the distal fiber tip is in a saline environment during lithotripsy due to improved index matching.
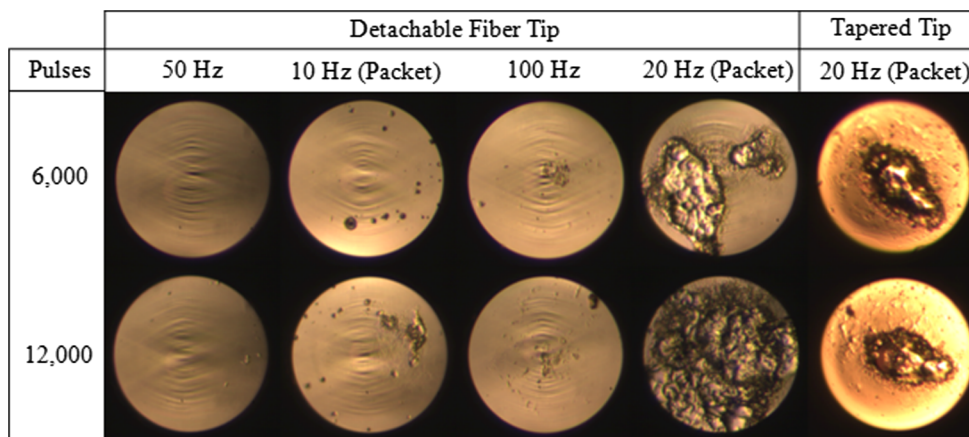

Fig. 8 Distal fiber tip degradation as a function of pulse profile and total number of pulses. All fiber tips were held manually in contact with the stone during laser irradiation with a 30-mJ pulse energy. Considerable fiber tip degradation was observed using the 20-Hz (Packet) pulse profile for both fibers.

Table 2 shows that the temperature rise in both fibers was a function of total pulses per second rather than the specific pulse configuration. The detachable fiber tip device did not reach a surface temperature above 50°C, which could be potentially harmful to the patient if in contact with soft tissues. The heat generated at the detachable distal fiber tip was believed to be the result of an inadvertent, slightly angled fiber tip surface, which resulted from polishing the short length fiber tips in fiber holders designed for much longer fibers. Steeper-angled tips divert more back reflection into the cladding of the fiber, causing more heat buildup. The tapered fibers were flat-polished by the manufacturer. The detachable interface heating was due to the reflections within the air gap region between the two fibers and the back-reflected light from the distal tip overfilling the trunk fiber upon return. An index-matching fluid may reduce this heating; however, no such fluid, which was biocompatible and provided a high optical damage threshold, was available. These thermal profiles were taken in air. During lithotripsy, the fibers would be in a saline irrigation environment providing cooling, and the distal fiber tip would have a silica/saline interface, thus reducing back reflection, which is believed to be the primary cause of the undesirable heating. However, both the detachable and the tapered fiber tips would be extruded from the ureteroscope during stone ablation, making the distal tip heating less significant than the detachable fiber tip interface which could remain inside the ureteroscope working channel.

The spatial beam profiles, as shown in Fig. 7, taken at the fiber tip surfaces show that the detachable fiber tip does not alter the shape of the Gaussian laser beam profile that was launched into the trunk fiber. However, the width of the beam does increase to better fill the larger tip diameter. This was predicted as there are no beam-altering surfaces; only two step-index fibers with identical NA. The spatial beam profiles, like the thermal measurements, were taken in air, and therefore, the outer ring visible in the tapered fiber profile could be an artifact of the distal fiber tip back-reflection re-encountering the tapered region from the opposite direction and then exiting the fiber tip. In saline, this outer ring may be reduced so that the actual spatial beam profile only contains the central region.

The under-filled proximal fiber NA (0.037) eventually expanded due to fiber bending to (0.078) after 2 m. The laser was also coupled slightly off-angle into the fiber's proximal end to avoid excessive back-reflection into the TFL, possibly leading to the increase in NA at the distal tip. However, the tapered distal fiber tip has a smaller numerical aperture (0.055) than that of the detachable fiber tip. This is due to the change in modal structure and focusing in the tapered region. The farfield spatial beam profiles are less significant to lithotripsy than the surface profiles. However, since cavitation bubbles serve as a conduit for the laser energy to the stone, the divergence or NA might play a small role in energy density as the light reaches the stone surface depending upon the fiber's distance to the stone, which is not constant. Therefore, the tapered fiber still offers a slight advantage over straight fibers because the energy density or spatial beam size is more uniform beyond the fiber distal tip.

4.3 Lithotripsy Analysis

Since COM urinary stones are the most common stone type operated upon, they were used to demonstrate a functional and practical prototype for a detachable fiber tip. Table 3 shows an increase in stone ablation rates for both the detachable and tapered fiber tips when using pulse packets versus standard pulse configurations. This is comparable to previous studies with a 100-μm-core diameter fiber operating at 35 mJ with a pulse width of 500 μs, which demonstrated COM stone ablation rates of 60 and 122 μg/s for the 50 and 10 Hz (Packet) profiles, respectively.[9] Although the energy density is lower in the detachable fiber tip, the same trend of nearly double the stone ablation rate still applies; the rates are only slightly lower. Added precautions were taken when handling the tapered fibers because the tapered fiber region was much more delicate and prone to breaking than the detachable fiber tip device. Slight differences in stone ablation rates between the detachable and tapered fiber tips could therefore be a result of less aggressive and less frequent contact force between the tapered fiber tip and the stone surface. Again, no statistical difference was seen between tapered and detachable fiber tip stone ablation rates.

TFL lithotripsy with low pulse energies and high-pulse rates resulted in stone vaporization or dusting with very small particle sizes created, rather than fragmentation into larger stone pieces. The laser stone vaporization approach may offer some advantages compared to fragmentation because the residual stone or dust particles are small enough to be naturally passed on their own, and unlike larger stone fragments, would not require use of a stone basket to retrieve fragments and ensure that the patient is stone-free. Further investigations comparing laser stone vaporization to fragmentation are warranted.

4.4 Degradation Analysis

Distal fiber tip degradation, as shown in Fig. 8, appeared to follow the same trend as the stone ablation rates. The packet configurations degraded the fiber tip faster than the equivalent standard pulse rate. The rapid heating of the fiber tip when in contact with the stone using the pulse packets or any high-pulse rate could be the cause of the fiber tip burn-back. It is possible that when a cavitation bubble forms between the fiber tip and stone surface, in contact, the first pulse voids the intermediate region of liquid and the following pulses in the packet arrive before collapse and therefore superheat the fiber tip and stone surface in the steady vapor pocket. When the fiber tip is slightly out of contact, operating at a lower pulse rate, or if the fiber has a smaller diameter, the cavitation bubble can collapse providing cooling to the fiber tip.

A previous study with 100-μm-core diameter fibers reported a decrease in fiber tip degradation or burn-back when using pulse packets.[9] The discrepancy in that study can be explained by the difference in ablation crater shapes caused by the pulse packet, which are much wider because of the increased ablation rate. The wider crater combined with the smaller fiber diameter could account for the better cooling. Standard pulse rate craters are more narrow and deep causing the small fiber to descend and get stuck. In these confined craters, the cavitation bubbles may not be able to collapse, resulting in superheating and faster fiber degradation. The detachable fiber tip has roughly 10 times the surface area of the 100-μm-core diameter fiber used previously as well as originating from separate manufacturers; therefore, the burn-back analysis is not directly comparable, and a more thorough study is warranted in the future. The tapered fiber tip showed similar degradation to the detachable fiber tip at 20 Hz (Packet); however, it was mostly confined to the central region of the tapered fiber. Assuming the outer ring in the tapered fiber's spatial beam profile, as shown in Fig. 7, is

reduced when operating in a saline environment, the beam central region closely resembled the degradation area of the fiber tip.

The distal fiber tip appeared to experience no or minimal burn-back at a standard pulse rate of 50 Hz, and therefore minimal heating of the fiber tip. This pulse rate was then used as a control model to observe whether or not the stone fragmentation and bombardment of the fiber tip with stone debris actually degraded the fiber. After 60,000 pulses, or 20 min of contact-stone ablation at 50 Hz, the roughness parameters of the fiber tip's surface, as shown in Fig. 9, were essentially unchanged. This result supports the conclusion that the urinary stone material is either not abrasive to the silica fiber or the debris created during TFL is smaller than the original fiber polishing grit size. In analogy to the photo-thermal mechanism used for stone ablation, degradation is instead primarily caused by the heating of the fiber tip until the silica undergoes a phase change.

5 Conclusions

The conventional Ho:YAG laser lithotripter cannot efficiently couple its laser energy into small fibers without proximal fiber tip damage, so instead, larger fibers are used, resulting in reduced ureteroscope deflection and irrigation rates. This study expands upon the potential benefits of using a TFL, which, with its single mode spatial beam profile, can efficiently couple its laser energy into smaller diameter fibers. With no proximal fiber tip damage, the primary motivation for using detachable fiber tips is the observation that only the distal fiber tip degrades or experiences fiber burn-back during stone fragmentation. This study introduced a novel, low-profile, twist-locking, spring-loaded, detachable distal fiber tip interface for potential use in TFL lithotripsy. A 1.00-mm OD detachable fiber tip interface was designed, constructed, and tested on urinary stones, *ex vivo*. Similar stone ablation rates between the previously studied tapered distal fiber tip and the detachable fiber tip were shown. The largest ablation rates were observed when using the pulse packets; however, higher rates also contributed to the fastest distal fiber tip degradation. For urologists desiring faster TFL lithotripsy procedures, use of detachable distal fiber tips may allow for rapid replacement of damaged fiber tips, without concern about the laser-to-trunk fiber connection.

References

1. J. Y. Clark, I. M. Thompson, and S. A. Optenberg, "Economic impact of urolithiasis in the United States," *J. Urol.* **154**(6), 2020–2024 (1995).
2. G. J. Vassar et al., "Holmium:YAG lithotripsy: photothermal mechanism," *J. Endourol.* **13**(3), 181–190 (1999).
3. S. Griffin, "Fiber optics for destroying kidney stones," *Biophoton. Int.* **11**(4), 44–47 (2004).
4. A. J. Marks et al., "Holmium:Yttrium-Aluminum-Garnet lithotripsy proximal fiber failures from laser and fiber mismatch," *Urol.* **71**(6), 1049–1051 (2008).
5. B. E. Knudsen et al., "Durability of reusable Holmium:YAG laser fibers: a multicenter study," *J. Urol.* **185**(1), 160–163 (2011).
6. R. L. Blackmon, P. B. Irby, and N. M. Fried, "Holmium:YAG ($\lambda = 2,120$ nm) versus Thulium fiber ($\lambda = 1,908$ nm) laser lithotripsy," *Lasers Surg. Med.* **42**(3), 232–236 (2010).
7. N. J. Scott, C. M. Cilip, and N. M. Fried, "Thulium fiber laser ablation of urinary stones through small-core optical fibers," *IEEE J. Sel. Top. Quantum Electron.* **15**(2), 435–440 (2009).
8. R. L. Blackmon, P. B. Irby, and N. M. Fried, "Thulium fiber laser lithotripsy using tapered fibers," *Lasers Surg. Med.* **42**(1), 45–50 (2010).
9. R. L. Blackmon, P. B. Irby, and N. M. Fried, "Enhanced Thulium fiber laser lithotripsy using micro-pulse train modulation," *J. Biomed. Opt.* **17**(2), 028002 (2012).
10. N. M. Fried, "Thulium Fiber Laser Lithotripsy: An *in vitro* analysis of stone fragmentation using a modulated 110-W Thulium fiber laser at 1.94 *μ*m," *Lasers Surg. Med.* **37**(1), 53–58 (2005).
11. R. L. Blackmon, P. B. Irby, and N. M. Fried, "Comparison of Holmium: YAG and thulium fiber laser lithotripsy: Ablation thresholds, ablation rates, and retropulsion effects," *J. Biomed. Opt.* **16**(7), 071403 (2011).
12. K. T. Schomacker et al., "Co:MgF2 laser ablation of tissue: Effect of wavelength on ablation threshold and thermal damage," *Lasers Surg. Med.* **11**(2), 141–151 (1991).
13. G. M. Hale and M. R. Querry, "Optical constants of water in the 200 nm to 200 *μ*m wavelength region," *Appl. Opt.* **12**(3), 555–563 (1973).
14. E. D. Jansen et al., "Temperature dependence of the absorption-coefficient of water for midinfrared laser radiation," *Lasers Surg. Med.* **14**(3), 258–268 (1994).
15. B. I. Lange, T. Brendel, and G. Hüttmann, "Temperature dependence of light absorption in water at holmium and thulium laser wavelengths," *Appl. Opt.* **41**(27), 5797–5803 (2002).
16. A. Vogel, P. Schmidt, and B. Flucke, "Minimization of thermomechanical side effects in IR ablation by use of multiply Q-switched laser pulses," *Med. Laser Appl.* **17**(1), 15–20 (2002).
17. D. P. Joseph et al., "A new and improved vitreoretinal erbium:YAG laser scalpel; long-term morphologic characteristics of retinal-choroidal injury," *Ophth. Surg. Las. Imag.* **35**(4), 304–335 (2004).
18. B. E. Knudsen et al., "Performance and safety of Holmium:YAG laser optical fibers," *J. Endourol.* **19**(9), 1092–1097 (2005).
19. A. C. Mues, J. M. Teichman, and B. E. Knudsen, "Quantification of Holmium:Yttrium aluminum garnet optical tip degradation," *J. Endourol.* **23**(9), 1425–1428 (2009).
20. J. P. Clarkin, R. J. Timmerman, and J. H. Shannon, "Shaped fiber tips for medical and industrial applications," *Proc. SPIE* **5317**, 70–80 (2004).
21. N. J. Scott et al., "Mid-IR germanium oxide fibers for contact erbium laser tissue ablation in endoscopic surgery," *IEEE J. Sel. Top. Quan. Electron.* **13**(6), 1709–1714 (2007).